A Universal Model for Spray Characteristics of Technical Diesel Sprays

G.Renner and R.R.Maly

Daimler-Benz AG
Aero- and Thermodynamics, FIM/T, D-70546 Stuttgart
Code G206
Germany

ABSTRACT

This paper describes a universal correlation model for simultaneous and assumption-free prediction of the temporal evolution of spray penetration, spray tip speed, spray angle, Sauter Mean Diameter and mean equivalance ratio of technical diesel nozzles - i.e. multi hole and/or pintle nozzles with flats - under realistic and instationary conditions. The model predicts all spray parameters with a single universal set of constants for arbitrary operating conditions (fuel and gas properties, pressure history of fuel line, needle lift, chamber back pressure and type of injector).

For the experimental verification of the model, detailed studies were carried out on non-evaporating diesel fuel sprays in a high pressure chamber at room temperature. The global spray parameters were measured by high-speed shadowgraphy. Droplet data were determined by a fast extinction scattering method and the Sauter Mean Diameter was measured with a Malvern instrument at various locations in the spray.

A very good agreement is obtained between computed and experimental data for a wide set of operating conditions and for inherently different commercial injector geometries.

INTRODUCTION

Spray formation controls ignition, combustion, pollutant formation (especially NO and PM) and noise of a diesel engine. Although there have been many attempts to predict fuel sprays, most of them focused on steady state conditions using lab-type injectors. So far only few models [1,2,3,4] consider time dependent fuel flow rates and line pressures, which are relevant for engine applications. Thus almost all available spray models are still unable to adequately predict essential spray characteristics (spray tip penetration, tip speed, spray cone angle, Sauter Mean Diameter and mean equivalance ratio) of technical sprays under realistic engine-like conditions without ad hoc adjustments of model "constants". Therefore, a universal analytical model based on modified correlation functions has been developed for simultaneous prediction of all spray parameters of commercial injectors for both DI and IDI engines. The model uses a single set of constants for all cases.

MATHEMATICAL MODEL

Subsequently the building blocks of the model are briefly described. An extensive discussion of the spray model can be found elsewhere [5].

Tip penetration

This block is based on the analytical model for spray tip penetration developed by Varde [6] for lab-type single hole nozzles operated under stationary conditions:

$$S = K \cdot A_1^{\alpha_1} \cdot A_2^{\alpha_2} \cdot A_3^{\alpha_3} \cdot A_4^{\alpha_4} \cdot A_5^{\alpha_5} \cdot \left(\frac{t}{t_0}\right)^{\alpha_t} \qquad (1)$$

The dimensionless coefficient A_1 accounts for the flow through a nozzle hole being characterized by its Reynolds number. Δp is the pressure drop across the length l of the hole, ρ_l and η_l are density and dynamic viscosity of the fuel, resp., and d_{eff} is the effective hydraulic diameter due to flow contraction. It is slightly smaller than the corresponding geometrical hole diameter d:

$$A_1 = \frac{\Delta p \cdot \rho_l \cdot d_{eff}^2}{\eta_l^2} \approx \mathrm{Re}^2 \qquad (2)$$

The dimensionless coefficient A_2 represents the Ohnesorge-number characterizing the resistance of the fuel to disintegrate into droplets:

$$A_2 = \frac{\rho_l \cdot \sigma_l \cdot d}{\eta_l^2} = \frac{1}{\mathrm{Oh}^2} \qquad (1)$$

σ_l = surface tension of the liquid (fuel).

The dimensionless coefficient A_3 accounts for the density ratio of the liquid and the gas phases:

$$A_3 = \frac{\rho_l}{\rho_g} \quad . \qquad (2)$$

The dimensionless coefficient A_4 represents the geometry of the nozzle hole:

$$A_4 = \frac{l}{d} \quad . \qquad (3)$$

Following considerations by Ranz [7], the viscosity ratio of liquid to gas phase during spray breakup is condensed into a dimensionless coefficient A_5:

$$A_5 = \frac{f_l}{f_g} = \frac{\eta_l}{\eta_g} \quad . \qquad (4)$$

The model constants were chosen from best square fits of correlation functions to extensive sets of experimental spray data measured on commercial injectors (see RESULTS):

$\alpha_1 = 0.3$ $\alpha_2 = -0.008$ $\alpha_3 = 0.2$

$\alpha_4 = 0.16$ $\alpha_5 = 0.6$ $\alpha_t = 0.4$.

The constant K in Eq. 1 depends slightly on the type of injector and serves for correcting minor differences in flow contraction (<9%) occurring in widely different geometries of technical nozzles:

$K = K_h = 0.065$ for hole nozzles and

$K = K_p = 0{,}069$ for pintle nozzles.

In short Eq. 1 can also be written as:

$$S_j = K_{vj} \cdot t^{\alpha_t} \qquad (5)$$

with K_{vj} being the Varde-"constant" and j= index for the type of nozzle. It should be noted however, that K_{vj} is by no means a constant in a proper sense but varies as function of the momentary values of injection and chamber pressure, valve lift, temperature and pressure of liquid and gas phase, fuel composition etc..

In Eq. 3 the fuel pressure drop Δp across the hole and the effective hole diameter d_{eff} are still unknowns. They are determined from a simplification of the nozzle geometry to 2 orifices, a central chamber and 2 plenums connected in series as shown in Fig. 1. From the continuity equation it follows for the fuel pressure p_{Sa} in the central chamber:

$$p_{Sa} = \left[\frac{\left(\frac{\mu_{Si} \cdot A_{Si}}{\mu_{Lo} \cdot A_{Lo}} \right)^2 + \frac{p_g}{p_L}}{1 + \left(\frac{\mu_{Si} \cdot A_{Si}}{\mu_{Lo} \cdot A_{Lo}} \right)^2} \right] \cdot p_L \cdot \qquad (8)$$

with A_{Si} the seat area and A_{Lo} the cross sectional area of the hole; p_g the back pressure and p_L the fuel line pressure.

The discharge coefficients of the nozzle hole μ_{Lo} and the seat μ_{Si} are determined from the known total pressure drop across the whole injector and its effective overall discharge coefficient μ_{ges}. For a hole nozzle the discharge coefficient μ_{Lo} is given by:

$$\left(\frac{1}{\mu_{ges} A_{Lo}} \right)^2 - \left(\frac{1}{\mu_{Lo} A_{Lo}} \right)^2 = \left(\frac{1}{\mu_{Si} \cdot A_{Si}} - \frac{1}{\mu_{Sa} \cdot A_{Sa}} \right)^2 \qquad (6)$$

with μ_{Sa} the discharge coefficient of the sac hole.

For a pintle nozzle μ_{Lo} is described by:

$$\left(\frac{1}{\mu_{ges} A_{Lo}} \right)^2 - \left(\frac{1}{\mu_{Lo} A_{Lo}} \right)^2 = \left(\frac{1}{\mu_{Si} \cdot A_{Si}} \right)^2 \qquad (7)$$

According to measurements by Hardenberg [8] for needle lifts greater than 0.005 mm, the discharge coefficients μ_{Si} and μ_{Sa} are nearly constant and have a value of 1. For needle lifts between 0 and 0.005 mm, μ_{Sa} is already constant. Hiroyasu [2] finds thus for the discharge coefficient μ_{Si}:

$$\mu_{Si} \approx 195 \cdot h_N \qquad h_N \le 0.005\,mm\,. \qquad (8)$$

The last unknown is the effective flow area $\mu_{ges} A_{Lo}$ which must still be measured for each type of injector unless calculated values from 3D injector modeling are available [9,10]. Since the accuracy of these simulations is still not satisfactory, it is recommended to use measured values. Examples for measured and calculated values of a four hole nozzle and a pintle nozzle are shown in Fig. 2. The comparison reveals, that the initial fuel flux in a hole nozzle is determined by the needle lift and the late flux by the diameter of the hole, respectively, whereas in the pintle nozzle the flow is always controlled by the effective section of the ring annulus and the flat area.

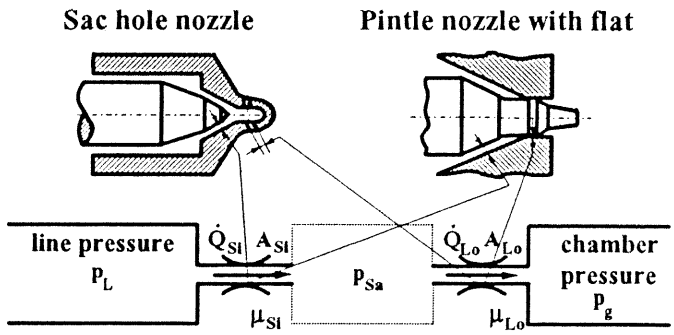

Fig. 1 Simplification of nozzle geometry used in the computation of discharge coefficients.

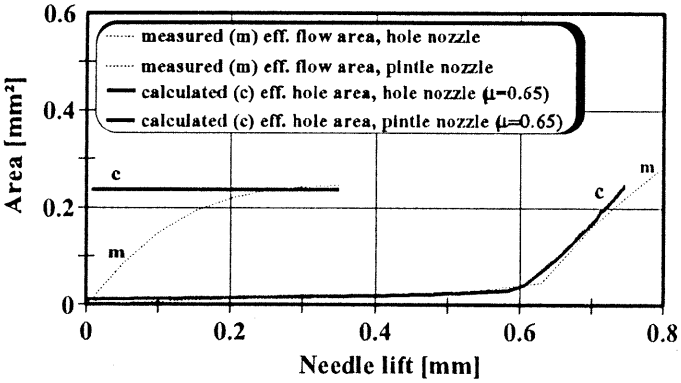

Fig. 2 Measured (m) effective flow areas and calculated (c) hole areas for a commercial four hole and a pintle nozzle, respectively.

Effective hole diameter of the pintle nozzle

In the model, arbitrary flow cross sections at different locations inside the nozzle are treated as circular cross sections with an equivalent effective geometrical area. Thus each section of the nozzle interior can be treated as a "hole nozzle". In Fig. 3 it is shown for a pintle nozzle to which degree of detail the nozzle geometry has to be broken down if a reasonable accuracy is to be achieved. For the computations in this paper the nozzle is divided into the flat area A_{Fl} and the ring annulus A_{Ring}. The total lift is divided into 4 part lifts (st_1, st_2, st_3, st_4).

The effective hole diameter is calculated accordingly as:

$$d_{eff} = \sqrt{\frac{4 \cdot (A_{Fl} + A_{Ring})}{\pi}}\,. \qquad (9)$$

Cone angle

Following Wakuri's analysis [11] the fuel spray may be treated as a mixture of fuel and entrained gas with a negligible relative velocity between fuel droplets and gas. For the time dependent cone angle Θ (e.g.: 1 ms after injection) Wakuri finds:

$$\Theta = 2 \cdot \arctan\left[\frac{v_{inj} \cdot d \cdot t_1}{\left(\rho_g/\mu \cdot \rho_l\right)^{1/2} \cdot S_1^2}\right] \quad (10)$$

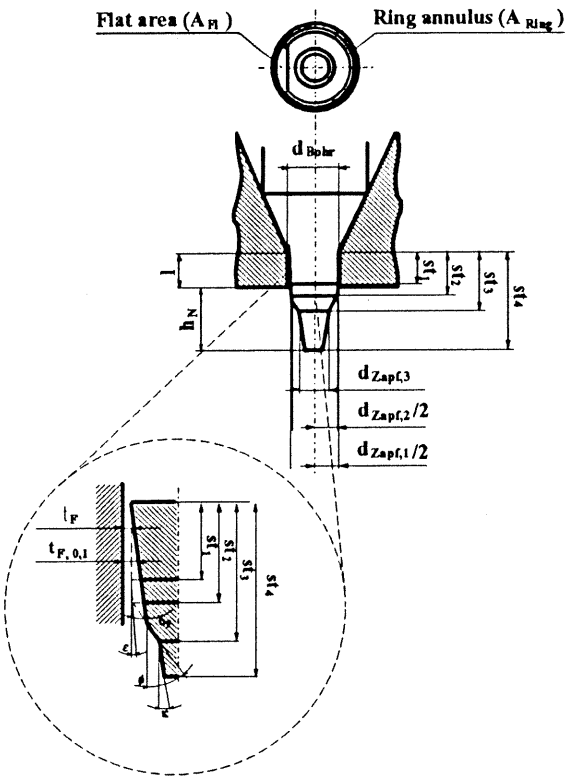

Fig. 3 Pintle nozzle with flat showing details of the different cross sections in the flat region.

Our experimental results indicate that the original density exponent of 1/2 is too large. A good fit is obtained only if the same exponent is used for all density ratios in the model, i.e. α_3 (see coefficient A_3 above). Hence we use the modified correlation:

$$\Theta = 2 \cdot \arctan K_W \cdot \left[\frac{v_{inj} \cdot d \cdot t_1}{\left(\rho_g/\mu \cdot \rho_l\right)^{\alpha_3} \cdot S_1^2}\right] \quad (11)$$

with the injection velocity v_{inj}:

$$v_{inj} = \sqrt{\frac{2 \cdot \Delta p}{\rho_l}} \quad (12)$$

and $K_W = 2.65$ $\mu = 0.65$ (discharge coefficient)
$t_1 = 1$ ms S_1= tip penetration at 1 ms.

Equivalance ratio

This is again modeled according to the analysis of the spray angle by Wakuri [11]. The excess air ratio (inverse of equivalance ratio), e.g. at 1 ms after injection, is given by:

$$\lambda_{L,K} \cong \frac{\tan\Theta}{L_{th} \cdot \sqrt{\mu}} \cdot \left(\frac{\rho_g}{\rho_l}\right)^{\alpha_3} \cdot \frac{S_1}{d} \quad (13)$$

with L_{th} = A/F ratio = 14.5 kg/kg for diesel fuel.

Sauter Mean Diameter

In modeling the Sauter Mean Diameter we follow Hiroyasu's treatment [12]. The Sauter Mean Diameter is calculated as function of the parameters defined already for Eq. 1 (injection pressure, ambient pressure, fuel kinematic viscosity, surface tension and geometric nozzle diameter):

$$\frac{SMD}{d} = \max\left[\frac{SMD_{ic}}{d}, \frac{SMD_{co}}{d}\right] \quad (14)$$

with max. [ ] denoting the larger value of:

$$\frac{SMD_{ic}}{d} = 4.12\left[\frac{v_0 d \rho_l}{\eta_l}\right]^{0,12}\left[\frac{v_0^2 d \rho_l}{\sigma_l}\right]^{-0,75}\left(\frac{\eta_l}{\eta_g}\right)^{0,54}\left(\frac{\rho_l}{\rho_g}\right)^{0,18} \quad (15)$$

$$\frac{SMD_{co}}{d} = .38\left[\frac{v_0 d \rho_l}{\eta_l}\right]^{0,25}\left[\frac{v_0^2 d \rho_l}{\sigma_l}\right]^{-0,32}\left(\frac{\eta_l}{\eta_g}\right)^{0,37}\left(\frac{\rho_l}{\rho_g}\right)^{-0,47} \quad (16)$$

An inspection of Eq. 19 reveals for the whole injection period an increase in the Sauter Mean Diameter with increasing back pressure in the chamber. This effect has neither been shown by other workers in the field [13,14,15] nor was it ever observed in our own measurements. Also, this formulation appears to be in contrast to the reasonable expectation that a higher gas density should lead to a better spray disintegration due to the higher forces acting on the surface of the injected liquid. In response to our own measurements, the exponent of the density ratio in Eq. 19 was modified therefore from -0.47 to +0.11; the constant was modified from 0.38 to 0.023. Thus Eq. 19 was replaced by Eq. 20 which has now the form:

$$\frac{SMD_{co}}{d} = .023\left[\frac{v_0 d \rho_l}{\eta_l}\right]^{0,25}\left[\frac{v_0^2 d \rho_l}{\sigma_l}\right]^{-0,32}\left(\frac{\eta_l}{\eta_g}\right)^{0,37}\left(\frac{\rho_l}{\rho_g}\right)^{0,11} \quad (17)$$

NUMERICAL SOLUTION

Since the line pressure is time dependent in technical injections, parcels of liquid, injected at different increments of time, show widely different velocities. This different behavior of instationary sprays over stationary ones must be accounted for appropriately. Therefore, the whole injection process is subdivided into a large but finite number of individual spray parcels having individual properties. Each parcel interacts with different conditions in the spray due to the interactions with its predecessors. This is modeled in the following way:

Each parcel leaves the nozzle with its unique initial velocity according to the momentary value of the Varde constant (see Eq. 7). Pertinent line pressures and effective hole diameters, resp., are used in computing the constant. The parcel propagates then in the wake of the spray tip, consisting of droplets and entrained air, moving at a mean velocity approximately equal to the tip velocity. The moving parcel is treated as if it were propagating into quiescent air (i.e. as the parcel at the tip) but with a modified velocity:

$$v_{p,\,eff} = v_{parcel} + v_{spray}$$

It suffers also deceleration and all other effects occurring in the viscous gas phase, all of which are integrated into the Varde model. Thus a parcel will steadily slow down but may still be faster than the spray tip and take over the tip position or it may be too slow to ever catch up. In this case it settles somewhere in the interior of the spray. The numerical algorithm for simultaneously solving all the equations above for a given number of parcels is based on the following assumptions:

- The whole spray is divided into n parcels
- Injection is divided into m time intervals
- The parcel at the spray tip moves into quiescent gas
- Each parcel inside the spray moves with $v_{p,eff}$
- The mean spray velocity is identical to the tip velocity
- Each parcel leaves the nozzle with its unique velocity
- Faster parcels pass slower parcels
- At each time step a new parcel is started, the positions of all parcels are updated and the parcel taking the tip position is calculated

According to Eq. 7 for each parcel j the following equations for the individual tip penetration and its relative tip speed hold:

$$S_j = K_{vj} \cdot t^{\alpha_t} \tag{18}$$

$$\dot{S}_j = \alpha_t \cdot K_{vj} \cdot t^{\alpha_t - 1} \tag{19}$$

In the short time interval Δt the variable gas velocity in the inner part of the spray is given by the expression:

$$\bar{v}_{j_0,i} = \frac{1}{i\Delta t - (i-1)\Delta t} \cdot \int_{(i-1)\Delta t}^{i\Delta t} \alpha_t \cdot K_{vj_0} t^{\alpha_t - 1} dt$$

$$\bar{v}_{j_0,i} = K_{vj_0} \cdot \Delta t^{\alpha_t - 1} \left\{ i^{\alpha_t} - (i-1)^{\alpha_t} \right\}. \tag{20}$$

The speed of parcel j is given by:

$$\bar{v}_{j,i} = K_{vj} \cdot \Delta t^{\alpha_t - 1} \left\{ (i-j+1)^{\alpha_t} - (i-j)^{\alpha_t} \right\} \tag{21}$$

and the penetration distance by:

$$S_{j,i} = S_{j,i-1} + \left(\bar{v}_{j,i} + \bar{v}_{j_{Sp},i} \right) \cdot \Delta t. \tag{22}$$

Based on these assumptions and equations the computational procedure is:

1. Compute the tip parcel ($j = j_{Sp}$) having max. ($S_{j,i}$)
2. Compute the actual gas speed as the speed of the tip parcel (Eq. 25)
3. Compute all parcel velocities with Eq. 25 for the ith time step: $i\Delta t$
4. Compute the effective parcel velocity for the ith time step $i\Delta t$ by:

$$\bar{v}^{eff}_{j,i} = \bar{v}_{j,i} + \bar{v}_{j_{Sp},i} \tag{23}$$

5. Compute the new positions of all parcels by Eq. 26
6. Increase i and redo the computation until $i = i_{end}$.

Good results were obtained for n = m = 250 parcels and time intervals, respectively.

EXPERIMENTAL

Spray penetration was measured in a high pressure chamber with four quartz windows on each side using high speed shadowgraphy (40.000 fps, up to 80 frames/injection, frame size 50x50 mm^2) with spark light sources and electronic image processing. The chamber was pressurized with N_2 at room temperature. The pressure was varied from 1 to 50 bars, corresponding to about 2.5 to 125 bar in a diesel engine. Only commercial injection equipment, injectors and engine-like operating conditions were used. Multi-hole nozzles were fitted with a specially designed skimmer to select a single hole for measurements without affecting operating conditions. A special line valve was used allowing single injections to be made without affecting pressure wave propagation in the fuel line and/or residual pressure. Droplet size and number density were determined by a very fast extinction scattering method [16]. The Sauter Mean Diameters were measured 20 mm below the injector tip and 2 mm off axis by a Malvern instrument with the laser beam reduced to a diameter of only 2 mm. The measurements were made up to a maximum of 50% obscuration to avoid erroneous data [17]. A description of the experimental details can be found elsewhere [3].

RESULTS AND DISCUSSION

An extensive experimental study of non-evaporating sprays was carried out to determine model constants and to verify the full model. Parameters varied were: type of injector, injection pressure and pressure history, chamber back pressure, fuel type, viscosity of fuel and hole sizes. Due to space limitations only a few characteristic results can be shown here. A complete set may be found elsewhere [5]. Generally a very good agreement was found between measurements and computations of all spray parameters. This is especially noteworthy for the time dependent variation of the cone angle, which still has to be assumed in many 3D spray models, and for the position of the discontinuity and the shape of the spray penetration of pintle nozzles. To the knowledge of the authors these computations are the first correct predictions for commercial pintle nozzles available. Line pressure and needle lift traces are shown in Figure 4. The effect of changing injector type, chamber back pressure, fuel type and hole diameter are shown in Figs. 5,6,7,8,9. Figure 10 demonstrates for the SMD the degree of agreement which is achieved between measurements and computations.

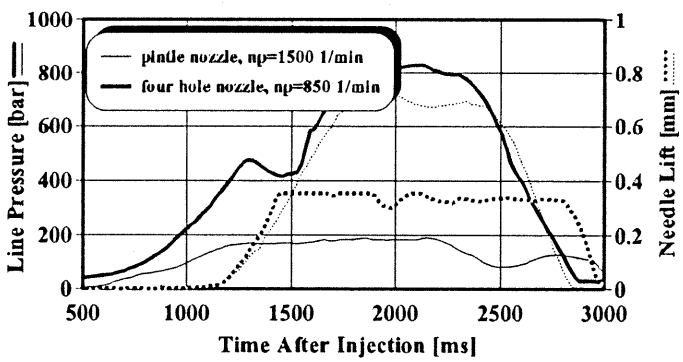

Fig. 4 Typical needle lift and line pressure traces for the different type of injectors.

CONCLUSIONS

1. Based on modified correlation functions, it is possible to compute: spray penetration, tip velocity, spray angle, mean excess air ratio and SMD for non evaporating technical sprays of commercial injectors with very good accuracy.
2. The spray structure depends essentially on the time dependent line pressure and the details of the inside geometry of the injector which control the time dependent effective cross sections for fuel flow by the needle lift. Quasi stationary models cannot predict these time dependent effects.

3. Correlation models for spray properties in the literature have been tested against a large set of spray data obtained under engine-like conditions. Modifications of model constants and exponents have been worked out so that viscosity and density effects are now properly accounted for.

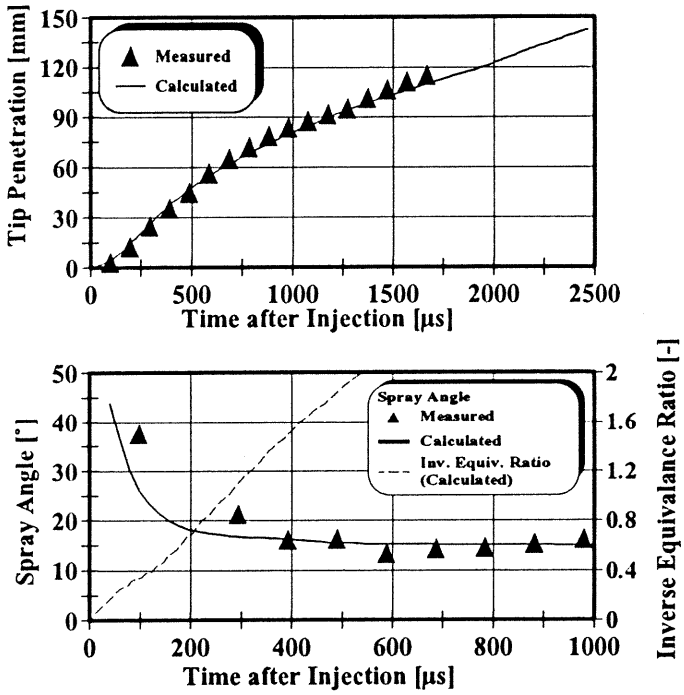

Fig. 5 Spray parameters for a commercial four hole nozzle; d = 0.34 mm; Line Pump; Pump Speed = 850 1/min; p_{max} = 850 bar; Q_i = 130 mm³/Stroke; Back Pressure = 27 bar; Fuel: Diesel.

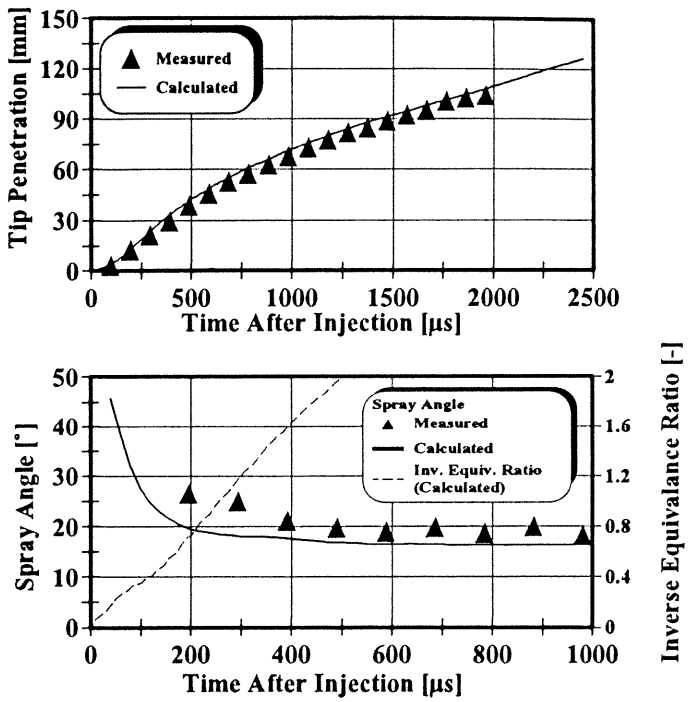

Fig. 7 Spray parameters for a commercial four hole nozzle; d = 0.34 mm; Line Pump; Pump Speed = 850 1/min; p_{max} = 850 bar; Q_i = 130 mm³/Stroke; Back Pressure = 45 bar; Fuel: Diesel.

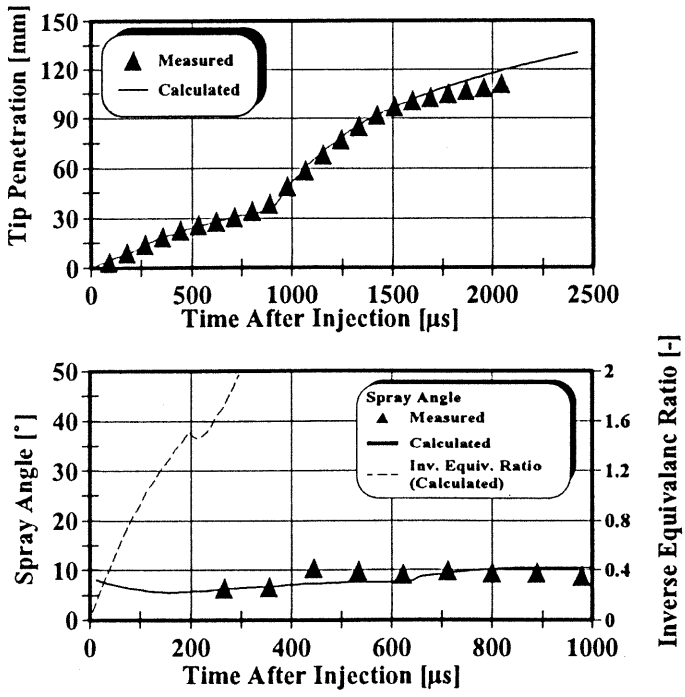

Fig. 6 Spray parameters for a commercial pintle nozzle with flat; Line Pump; Pump Speed = 1500 1/min; p_{max} = 180 bar; Q_i = 20 mm³/Stroke; Back Pressure = 25 bar; Fuel: Diesel.

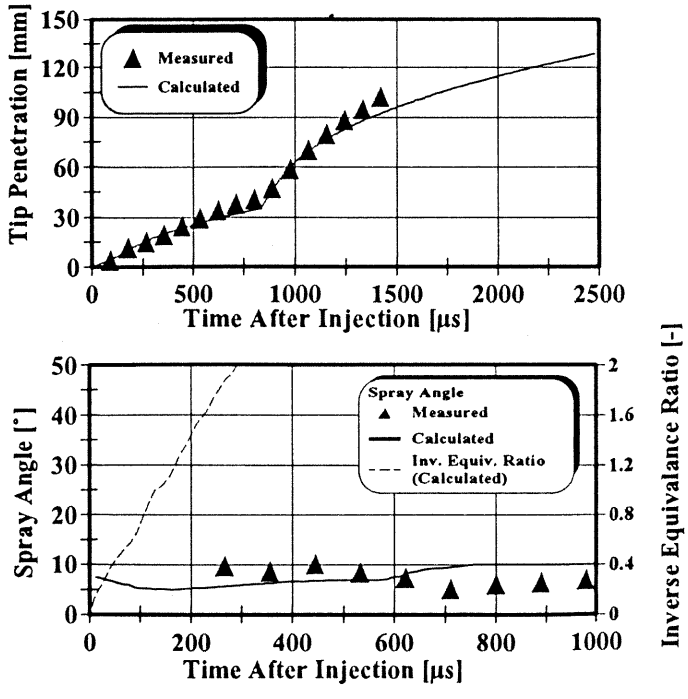

Fig. 8 Spray parameters for a commercial pintle nozzle with flat; Line Pump; Pump Speed = 1500 1/min; p_{max} = 180 bar; Q_i = 20 mm³/Stroke Back Pressure = 25 bar; Fuel: Rape Seed Oil.

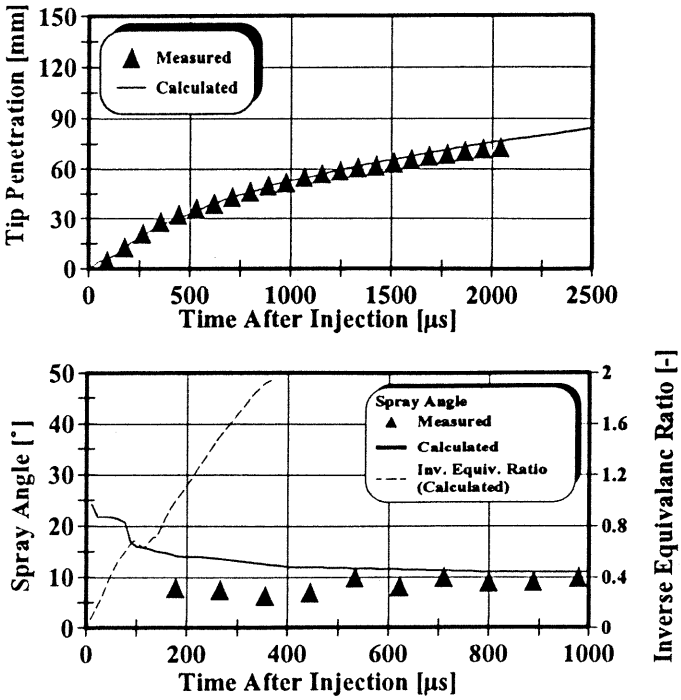

Fig. 9 Spray parameters for a commercial single hole nozzle ; d = 0.15 mm; Line Pump; Pump Speed = 1500 1/min; p_{max} = 350 bar; Q_i = 20 mm³/Stroke
Back Pressure = 25 bar; Fuel: Diesel.

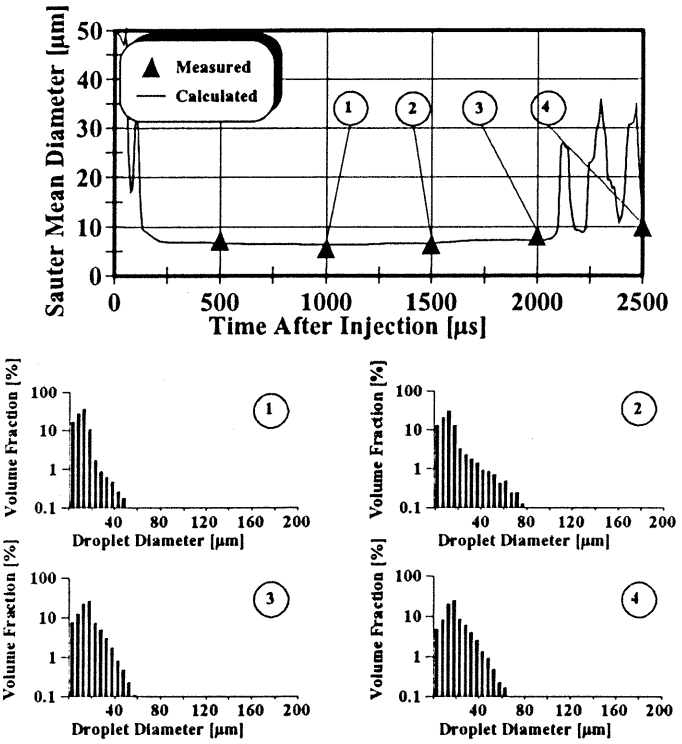

Fig. 10 Time history of the SMD of a single hole nozzle ; d = 0.15 mm; Line Pump; Pump Speed = 1500 1/min; p_{max} = 350 bar; Q_i = 20 mm³/Stroke;
Back Pressure = 25 bar; Fuel: Diesel.

4. The detailed instantaneous conditions in the spray - location and velocity of injected liquid, velocity of the mixture of droplets and entrained air inside the spray - must be used for computing spray formation.

REFERENCES

1. Janson, G., "Weiterentwicklung eines Modells zur Beschreibung des instationären Einspritz- und Ausbreitungsverhaltens von Dieselkraftstoffstrahlen bei realen Bedingungen", Thesis, University Kaiserslautern, 1990.
2. Xu, M., Nishida, K., Hiroyasu, H., "A Practical Calculation Method for Injection Pressure and Spray Penetration in Diesel Engines", SAE Paper 920624, 1992.
3. Nishida, K., Yoshisaki, T. and Hiroyasu, H., "Strategy to low NOx and Smoke Emissions by Simulation and Experiment", 20th CIMAC Congress, Paper D20, London 1993.
4. Manuel, A., Gonzalez, D., Lian, Z.W. and Reitz, R.D., "Modeling Diesel Spray Vaporization and Combustion", SAE Paper 920579, 1992.
5. Renner, G., "Experimentelle und rechnerische Untersuchungen über die Struktur technischer Dieseleinspritzstrahlen", VDI-Fortschrittbericht Reihe 12, 1994.
6. Varde, K.S. and Popa, D.M., "Diesel Fuel Spray Penetration at High Injection Pressures", SAE Paper 830448, 1983.
7. Ranz, W.E., "On Sprays and Spraying", Engineering Research Bulletin B-65, University of Pennsylvania, 1956.
8. Hardenberg, H. "Die Nadelhubabhängigkeit der Durchflußbeiwerte von Lochdüsen für Direkteinspritzdieselmotoren", MTZ Vol. 46, pp.143-146, 1985.
9. Oishi, Y., Miura, A., Hamazaki, N. and Watanabe, Y., "A Computational Study into the Effect of the Injection Nozzle Inclination Angle on the Flow Characteristics in Nozzle Holes", SAE Paper 920 580, 1992.
10. Date, K., Manabe, M., Kano, H. and Kato, M., "Contribution of Fuel Flow Improvement in Nozzle to Spray Formation", SAE Paper 920 622, 1992.
11. Wakuri, Y., Fujii, M., Amitani, T. and Tsuneya, R., "Studies on the Penetration of Fuel Spray in a Diesel Engine", Bulletin of JSME Vol. 3, 1960.
12. Hiroyasu, H., Arai, M. and Tabata, M., "Empirical Equations for the Sauter Diameter of a Diesel Spray", SAE Paper 890464, 1989.
13. Alloca, L., Belardini, P., Bertoli, C. Coricione, F.E. and De Angelis, F., "Experimental and Numerical Analysis of a Diesel Spray", SAE Paper 920576, 1992.
14. Gong, Y., You, L. and Liang, X., "An Investigation on Droplet Size Distribution and Evaporation of Diesel Fuel Sprays at High Injection Pressure by Using Laser Diagnostic Technique", SAE Paper 920090, 1992.
15. De Corso, S.M., "Effect of Ambient and Fuel Pressure on Spray Drop Size", Transactions of the ASME, 1960.
16. Maly, R.R., Mayer, G., Reck, B., and Schaudt, R.A., Optical Diagnostic for Diesel-Sprays with ms-Time Resolution, SAE Paper 910727, 1991.
17. Gülder, Ö.L., "Multiple Scattering Effects in Drop Sizing of Dense Fuel Sprays by Laser Diffraction, Combustion and Fuels in Gas Turbine Engines", AGARD-CP-422, 1987.